Commun Nonlinear Sci Numer Simulat 17 (2012) 1065–1084

Contents lists available at ScienceDirect

Commun Nonlinear Sci Numer Simulat

journal homepage: www.elsevier.com/locate/cnsns

Modeling and numerical simulation of linear and nonlinear spacecraft attitude dynamics and gravity gradient moments: A comparative study

M. Navabi [a], N. Nasiri [a], Mehdi Dehghan [b,*]

[a] Faculty of New Technologies Engineering, Shahid Beheshti University, G.C., Tehran, Iran
[b] Department of Applied Mathematics, Faculty of Mathematics and Computer Sciences, Amirkabir University of Technology, 424, Hafez Ave., Tehran, Iran

ARTICLE INFO

Article history:
Received 9 November 2010
Received in revised form 23 June 2011
Accepted 25 June 2011
Available online 7 July 2011

Keywords:
Linear and nonlinear modeling
Numerical simulation
Gravity gradient moment
Spacecraft attitude dynamics

ABSTRACT

In this paper linear and nonlinear models of spacecraft attitude dynamics equations and gravity gradient moments are investigated. In addition, effects of gravity gradient moments on attitude dynamics of the satellite are studied. The purpose of this paper is to present a comparison between nonlinear and linear models of spacecraft attitude dynamics and gravity gradient moments in order to determine divergence of linear approximation from the nonlinear model. Simulation results indicate that designer of spacecraft attitude control subsystem should be meticulous in applying linear approximation of equations especially in low earth orbits. Consequently, finding an upper bound for small angle to keep the linear model valid and precise enough would be a vital part of using linear approximation. Results supported by numerical examples demonstrate various features of this study.

1. Introduction

Today's modern satellites are expected to be more precise than their precedents to satisfy demanding mission requirements. Spacecraft attitude dynamics are described by the basic Euler's equations [1]. Exact solutions for attitude dynamics equations are complicated and highly nonlinear. However, it is often necessary to employ them in order to study the actual behavior of system dynamics.

The nonlinear dynamics equations are approximated, around a nominal operating condition, to obtain a linearized model. Linearized attitude equation is used in preliminary design, stability analysis and utilizing conventional classic control methods [2,3]. In addition, when the design problem allows working with principal axes, products of inertia can be eliminated from dynamic equations to simplify the equations [1]. Although linear attitude dynamics equations are frequently used in preliminary stages of design [4–6], linearization acts as a critical source of error in many cases.

The purpose of this paper is to present a comparison between nonlinear and linear models of spacecraft attitude dynamics equations and gravity gradient moments in order to determine the divergence of linear approximation from nonlinear model. A similar study on linear and nonlinear simulations of aircraft dynamics using body axis systems has been carried out [7].

In the current study, we emphasize the importance of employing either linear or nonlinear models of spacecraft attitude equations. In a further step, considering desired accuracy of the mission, error of linear approximation is presented as a metric to determine the upper bound for validating "small angle" assumption.

* Corresponding author.
E-mail addresses: civil.space.edu@gmail.com (M. Navabi), mdehghan@aut.ac.ir, mdehghan.aut@gmail.com (M. Dehghan).

1007-5704/$ - see front matter © 2011 Elsevier B.V. All rights reserved.
doi:10.1016/j.cnsns.2011.06.035

Here gravity gradient (GG) moments are considered as the external torque. Gravity gradient torque is inherent in low earth orbit (LEO) satellites and cannot be neglected in cases where attitude of spacecraft is passively controlled [1,8]. Thus, it is crucial to investigate linear and nonlinear equations of GG moments as well.

In this study, first of all, nonlinear spacecraft attitude equations and gravity gradient moments are derived. In the second step, linearized attitude equations and gravity gradient moments are obtained considering small angle assumption. Thirdly, numerical simulations of linear and nonlinear equations at the same step size are presented which illustrate divergence of linearized equation from nonlinear model. The error tendency is determined according to the increase in attitude angles. A similar comparison is done to evaluate effects of gravity gradient moments as well. According to numerical simulations and desired accuracy, validity of linear approximation is determined. Finally, linearization error percentage is presented as a metric for verifying the validity of "small angle" assumption through identifying an upper bound.

2. Spacecraft nonlinear attitude equations

It is necessary to develop basic concepts of satellite attitude equations before considering a specific problem. A rigid spacecraft can be described as a system of particles that their relative distances are fixed during time. Euler's moment equation is as follows [1]:

$$\mathbf{T} = \dot{\mathbf{h}}_I = \dot{\mathbf{h}}_B + \boldsymbol{\omega} \times \mathbf{h}_B, \tag{1}$$

where $\mathbf{T}$ denotes external moments vector, $\mathbf{h}$ is angular momentum vector, and $\boldsymbol{\omega}$ is angular velocity vector, and subscripts I and B refer to inertial and body frames respectively. To derive spacecraft attitude equations, the external moments are shown as sum of disturbance ($\mathbf{T_d}$) and control ($\mathbf{T_c}$) torques: $\mathbf{T} = \mathbf{T_c} + \mathbf{T_d}$ and total angular momentum as sum of rigid body ($\mathbf{h}_B$) and momentum exchange devices ($\mathbf{h}_w$): $\mathbf{h} = \mathbf{h}_B + \mathbf{h}_w$.

The basic reference frames are introduced before derivation of the equations. In Fig. 1, the inertial (I), orbital reference (R) and body (B) frames are shown. Center of the inertial frame is located on the earth's center of mass (CM), Z_I-axis is along earth's axis of rotation, X_I-axis points toward the vernal equinox and Y_I-axis completes a right handed frame.

The orbital reference frame is defined as follows; its origin moves with CM of the satellite in orbit while Z_R axis points toward CM of the earth and X_R-axis is in the plane of orbit, perpendicular to Z_R-axis, in the direction of velocity of spacecraft. Y_R-axis is normal to the local plane of orbit. The satellite body frame is defined by X_B, Y_B and Z_B and Euler angles are defined as rotational angles about body axes as follows: ψ about Z_B-axis, θ about Y_B-axis and ϕ about X_B-axis ($3 \rightarrow 2 \rightarrow 1$ rotation) [1].

The angular momentum ($\mathbf{h}$) is obtained by Eq. (2)

$$\mathbf{h} = [\mathbf{I}]\boldsymbol{\omega},$$

$$\mathbf{I} = \begin{bmatrix} I_{xx} & -I_{xy} & -I_{xz} \\ -I_{yx} & I_{yy} & -I_{yz} \\ -I_{zx} & -I_{zy} & I_{zz} \end{bmatrix}, \quad \boldsymbol{\omega} = \begin{bmatrix} \omega_x \\ \omega_y \\ \omega_z \end{bmatrix}, \tag{2}$$

where $\mathbf{I}$ represents tensor of inertia and $\boldsymbol{\omega}$ is angular velocity. Thus, the general attitude equation of a rigid spacecraft can be modeled by Eq. (3)

$$\begin{aligned} \sum T_x &= [\dot{h}_x + \dot{h}_{wx} + (\omega_y h_z - \omega_z h_y) + (\omega_y h_{wz} - \omega_z h_{wy})], \\ \sum T_y &= [\dot{h}_y + \dot{h}_{wy} + (\omega_z h_x - \omega_x h_z) + (\omega_z h_{wx} - \omega_x h_{wz})], \\ \sum T_z &= [\dot{h}_z + \dot{h}_{wz} + (\omega_x h_y - \omega_y h_x) + (\omega_x h_{wy} - \omega_y h_{wx})], \end{aligned} \tag{3}$$

where ω is angular velocity vector in body frame relative to inertial frame ($\omega = \omega_{BI}$), ω is sum of angular velocity vector of the reference frame relative to the inertial frame (ω_{RI}) and angular velocity of body frame relative to the reference frame (ω_{BR}), shown in Eq. (4)

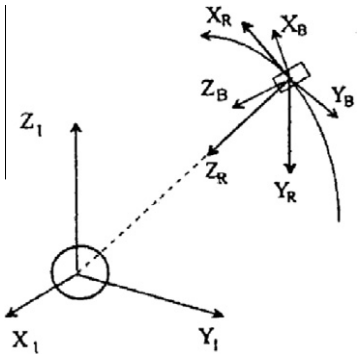

Fig. 1. Inertial (I), orbital reference (R) and body (B) frames.

$$\omega = \omega_{BI} = \omega_{RI} + \omega_{BR}. \tag{4}$$

Assuming a circular orbit, attitude kinematic equations are derived in Eqs. (5)–(8). Angular velocity vector of the reference frame relative to the inertial frame ($\omega_{RI} = [0\ -\omega_0\ 0]'$), is transformed into satellite's body frame using transformation matrix C:

$$\omega_{RI} = C \begin{bmatrix} 0 \\ -\omega_0 \\ 0 \end{bmatrix}, \tag{5}$$

$$C = \begin{bmatrix} \cos\theta\cos\psi & \cos\theta\sin\psi & -\sin\theta \\ -\cos\phi\sin\psi + \sin\phi\sin\theta\cos\psi & \cos\phi\cos\psi + \sin\phi\sin\psi\sin\theta & \sin\phi\cos\theta \\ \sin\phi\sin\psi + \cos\phi\sin\theta\cos\psi & -\sin\phi\cos\psi + \cos\phi\sin\theta\sin\psi & \cos\phi\cos\theta \end{bmatrix}, \tag{6}$$

where $\omega_0 = \sqrt{\frac{\mu}{R^3}}$ indicates angular velocity of the spacecraft in the circular orbit and $\mu = G \times M$ is gravitational parameter of the earth noting that G is universal gravitational constant. Also, M is mass of the spherical primary (for the earth $\mu = 3.986e14\ m^3/s^2$), and ϕ, θ, ψ *and* $\dot{\phi}, \dot{\theta}, \dot{\psi}$ denote roll, pitch, yaw angles and their rates, respectively.

Angular velocity of the body frame relative to the reference frame is given in Eq. (7)

$$\omega_{BR} = \begin{bmatrix} \dot{\phi} - \dot{\psi}\sin\theta \\ \dot{\theta}\cos\phi + \dot{\psi}\cos\theta\sin\phi \\ \dot{\psi}\cos\theta\cos\phi - \dot{\theta}\sin\phi \end{bmatrix}. \tag{7}$$

Substituting Eqs. (5) and (7) in Eq. (4), angular velocity vector in the body frame relative to the inertial frame is found by Eq. (8)

$$\omega = \begin{bmatrix} \dot{\phi} - \dot{\psi}\sin\theta - (\cos\theta\sin\psi)\omega_0 \\ \dot{\theta}\cos\phi + \dot{\psi}\cos\theta\sin\phi - (\cos\phi\cos\psi + \sin\phi\sin\theta\sin\psi)\omega_0 \\ \dot{\psi}\cos\theta\cos\phi - \dot{\theta}\sin\phi - (-\sin\phi\cos\psi + \cos\phi\sin\theta\sin\psi)\omega_0 \end{bmatrix}. \tag{8}$$

Complete nonlinear attitude equations in three axes are obtained by substituting Eq. (8) and its derivatives in Eq. (3), given in Eqs. (9)–(11). Nonlinear attitude equation on roll axis is presented in Eq. (9)

$$\begin{aligned} T_{cx} + T_{dx} = {} & (\ddot{\phi} - \ddot{\psi}\sin\theta - \dot{\psi}\dot{\theta}\cos\theta - (-\dot{\theta}\sin\theta\sin\psi + \dot{\psi}\cos\theta\cos\phi\omega_0)I_x - (\ddot{\theta}\cos\phi - \dot{\theta}\dot{\phi}\sin\phi + \ddot{\psi}\cos\theta\sin\phi \\ & + \dot{\psi}(-\dot{\theta}\sin\theta\sin\phi + \dot{\phi}\cos\theta\cos\phi - (\dot{\phi}\sin\phi\cos\psi - \dot{\psi}\cos\phi\sin\psi + \dot{\phi}\cos\phi\sin\theta\sin\psi \\ & + \sin\phi\dot{\psi}\dot{\theta}\cos\theta\cos\psi\omega_0)I_{xy} - (\ddot{\psi}\cos\theta\cos\phi + \dot{\psi}(-\dot{\theta}\sin\theta\cos\phi - \dot{\phi}\cos\theta\sin\phi) - \ddot{\theta}\sin\phi - \dot{\theta}\dot{\phi}\cos\phi \\ & - (\dot{\phi}\cos\phi\cos\psi + \dot{\psi}\sin\phi\sin\psi - \dot{\phi}\sin\phi\sin\theta\sin\psi + \cos\phi(\dot{\theta}\cos\theta\sin\psi + \dot{\psi}\sin\theta\cos\psi\omega_0)I_{xz} + \dot{h}_{wx} \\ & + (\dot{\theta}\cos\phi + \dot{\psi}\cos\theta\sin\phi - ((\cos\phi\cos\psi + \sin\phi\sin\theta\sin\psi)\omega_0)(\dot{\psi}\cos\theta\cos\phi - \dot{\theta}\sin\phi - (-\sin\phi\cos\psi \\ & + \cos\phi\sin\theta\sin\psi\omega_0)I_z - (\dot{\phi} - \dot{\psi}\sin\theta - \cos\theta\sin\psi\omega_0)I_{xz} - (\dot{\theta}\cos\phi + \dot{\psi}\cos\theta\sin\phi - (\cos\phi\cos\psi \\ & + \sin\phi\sin\theta\sin\psi\omega_0)I_{yz}) - \dot{\psi}\cos\theta\cos\phi - \dot{\theta}\sin\phi - (-\sin\phi\cos\psi\sin\theta\sin\psi\omega_0)(\dot{\theta}\cos\phi + \dot{\psi}\cos\theta\sin\phi \\ & - (\cos\phi\cos\psi + \sin\phi\sin\theta\sin\psi\omega_0)I_y - (\dot{\phi} - \dot{\psi}\sin\theta - \cos\theta\sin\psi\omega_0)I_{xy} - (\dot{\psi}\cos\theta\cos\phi - \dot{\theta}\sin\phi \\ & - (-\sin\phi\cos\psi + cos\phi\sin\theta\sin\psi)\omega_0)I_{yz} + (\dot{\theta}\cos\phi + \dot{\psi}\cos\theta\sin\phi - ((\cos\phi\cos\psi \\ & + \sin\phi\sin\theta\sin\psi)\omega_0)h_{wz} - (\dot{\psi}\cos\theta\cos\phi - \dot{\theta}\sin\phi - (-\sin\phi\cos\psi\cos\phi\sin\theta\sin\psi)\omega_0)h_{wy}. \end{aligned} \tag{9}$$

Also, nonlinear attitude equation on pitch axis is presented in Eq. (10)

$$\begin{aligned} T_{dy} + T_{cy} = {} & (\ddot{\theta}\cos\phi - \dot{\theta}\dot{\phi}\sin\phi + \dot{\psi}\cos\theta\sin\phi + \dot{\psi}(-\dot{\theta}\sin\theta\sin\phi + \dot{\phi}\cos\theta\cos\phi) - (-\dot{\phi}\sin\phi\cos\psi - \dot{\psi}\cos\phi\sin\psi \\ & + \dot{\phi}\cos\phi\sin\theta\sin\psi + \sin\phi\dot{\psi}\dot{\theta}\cos\theta\cos\psi\omega_0)I_y - (\ddot{\phi} - \ddot{\psi}\sin\theta - \dot{\psi}\dot{\theta}\cos\theta - (-\dot{\theta}\sin\theta\sin\psi \\ & + \dot{\psi}\cos\theta\cos\psi\omega_0)I_{xy} - (\ddot{\psi}\cos\theta\cos\phi + \dot{\psi}(-\dot{\theta}\sin\theta\cos\phi - \dot{\phi}\cos\theta\sin\phi) - \ddot{\theta}\sin\phi - \dot{\theta}\dot{\phi}\cos\phi \\ & - (-\dot{\phi}\cos\phi\cos\psi + \dot{\psi}\sin\phi\sin\psi - \dot{\phi}\sin\phi\sin\theta\sin\psi + \cos\phi(\dot{\theta}\cos\theta\sin\psi\dot{\psi}\sin\theta\cos\psi)\omega_0)I_{yz} \\ & + \dot{h}_{wy} + (\dot{\psi}\cos\theta\cos\phi - \dot{\theta}\sin\phi - (-\sin\phi\cos\psi + \cos\phi\sin\theta\sin\psi\omega_0)(\dot{\phi} - \dot{\psi}\sin\theta - \cos\theta\sin\psi\omega_0)I_x \\ & - (\dot{\theta}\cos\psi + \dot{\psi}\cos\theta\sin\phi - (\cos\phi\cos\psi + \sin\phi\sin\theta\sin\psi\omega_0)I_{xy} - (\dot{\psi}\cos\theta\cos\phi - \dot{\theta}\sin\phi \\ & - (-\sin\phi\cos\psi + \cos\phi\sin\theta\sin\psi)\omega_0)I_{xz} - (\dot{\phi} - \dot{\psi}\sin\theta - \cos\theta\sin\psi\omega_0)((\dot{\psi}\cos\theta\cos\phi - \dot{\theta}\sin\phi \\ & - (-\sin\phi\cos\psi + \cos\phi\sin\theta\sin\psi)\omega_0)I_z - (\dot{\phi} - \dot{\psi}\sin\theta - \cos\theta\sin\psi\omega_0)I_{xz} - (\dot{\theta}\cos\phi + \dot{\psi}\cos\theta\sin\phi \\ & - (\cos\phi\cos\psi + \sin\phi\sin\theta\sin\psi)\omega_0)I_{yz} + (\dot{\psi}\cos\theta\cos\phi - \dot{\theta}\sin\phi - (-\sin\phi\cos\psi \\ & + \cos\phi\sin\theta\sin\psi)\omega_0)h_{wx} - (\dot{\phi} - \dot{\psi}\sin\theta - \cos\theta\sin\psi\omega_0)h_{wz}. \end{aligned} \tag{10}$$

And nonlinear attitude equation on yaw axis is given in Eq. (11).

$$\begin{aligned}T_{dz}+T_{cz}=&(\ddot{\psi}\cos\theta\cos\phi+\dot{\psi}(-\dot{\theta}\sin\theta\cos\phi-\dot{\phi}\cos\theta\sin\phi)-\ddot{\theta}\sin\phi-\dot{\theta}\dot{\phi}\cos\phi-(-\dot{\phi}\cos\phi\cos\psi+\dot{\psi}\sin\phi\sin\psi\\&-\dot{\phi}\sin\phi\sin\theta\sin\psi+\cos\phi(\dot{\theta}\cos\theta\sin\psi+\dot{\psi}\sin\theta\cos\psi)\omega_0)I_z+(\ddot{\phi}-\ddot{\psi}\sin\theta-\dot{\psi}\dot{\theta}\cos\theta\\&-(-\dot{\theta}\sin\theta\sin\psi+\dot{\psi}\cos\theta\cos\psi)\omega_0)I_{xz}-(\ddot{\theta}\cos\phi-\dot{\theta}\dot{\phi}\sin\phi+\ddot{\psi}\cos\theta\sin\phi+\dot{\psi}(-\dot{\theta}\sin\theta\sin\phi\\&+\dot{\phi}\cos\theta\cos\phi)-(-\dot{\phi}\sin\phi\cos\psi-\dot{\psi}\cos\phi\sin\psi+\dot{\phi}\cos\phi\sin\theta\sin\psi+\sin\phi\dot{\psi}\dot{\theta}\cos\theta\cos\psi)\omega_0)I_{yz}\\&+\dot{h}_{wz}+(\dot{\phi}-\dot{\psi}\sin\theta-\cos\theta\sin\psi\omega_0)(\dot{\theta}\cos\phi+\dot{\psi}\cos\theta\sin\phi-(\cos\phi\cos\psi+\sin\phi\sin\theta\sin\psi)\omega_0)I_y\\&-(\dot{\phi}-\dot{\psi}\sin\theta-\cos\theta\sin\psi\omega_0)I_{xy}-(\dot{\psi}\cos\theta\cos\phi-\dot{\theta}\sin\phi-(-\sin\phi\cos\psi+\cos\phi\sin\theta\sin\psi)\omega_0)I_{yz}\\&-(\dot{\theta}\cos\phi+\dot{\psi}\cos\theta\sin\phi-(\cos\phi\cos\psi+\sin\phi\sin\theta\sin\psi)\omega_0(\dot{\phi}-\dot{\psi}\sin\theta-\cos\theta\sin\psi\omega_0)I_x\\&-(\dot{\theta}\cos\phi+\dot{\psi}\cos\theta\sin\phi-(\cos\phi\cos\psi+\sin\phi\sin\theta\sin\psi)\omega_0)I_{xy}-(\dot{\psi}\cos\theta\cos\phi-\dot{\theta}\sin\phi\\&-(-\sin\phi\cos\psi+\cos\phi\sin\theta\sin\psi)\omega_0)I_{xz}+(\dot{\phi}-\dot{\psi}\sin\theta-\cos\theta\sin\psi\omega_0)h_{wy}-(\dot{\theta}\cos\phi+\dot{\psi}\cos\theta\sin\phi\\&-(\cos\phi\cos\psi+\sin\phi\sin\theta\sin\psi)\omega_0)h_{wx}.\end{aligned}\tag{11}$$

2.1. Attitude equations linearization

Considering Eqs. (9)–(11), nonlinear model of attitude dynamics is highly nonlinear and complicated to work with. The nonlinear equations are linearized utilizing linearization methods around the equilibrium point. In order to linearize the nonlinear model, attitude angles are assumed small enough, therefore the cosine is approximately equal to 1 and the sine is approximated by the value of the angle, in radians. Utilizing this method and neglecting second order and higher terms, which are the products of two or more attitude angles or rates, linear approximations of attitude equations are presented in Eqs. (12)

$$\begin{aligned}T_{dx}+T_{cx}&=I_x\ddot{\phi}+(I_y-I_z)\omega_0^2\phi+(I_y-I_z-I_x)\omega_0\dot{\psi}+\dot{h}_{wx}-h_{wz}\omega_0-h_{wy}\dot{\psi}-h_{wy}\omega_0\phi\\&\quad-I_{xy}\ddot{\theta}-I_{xz}\ddot{\psi}-I_{xz}\omega_0^2\psi+2I_{yz}\omega_0\dot{\theta}-2I_{yz}\omega_0^2,\\T_{dy}+T_{cy}&=I_y\ddot{\theta}++\dot{h}_{wy}-I_{xy}(\ddot{\phi}-2\omega_0\dot{\psi}-\omega_0^2\phi)+I_{yz}(-\ddot{\psi}-2\omega_0\dot{\phi}+\omega_0^2\psi)+h_{wx}\dot{\psi}\\&\quad+h_{wx}\omega_0\phi-h_{wz}\dot{\phi}+h_{wz}\psi,\\T_{dz}+T_{cz}&=I_z\ddot{\psi}+(I_z+I_x-I_y)\omega_0\dot{\phi}+(I_y-I_z)\omega_0^2\psi+\dot{h}_{wz}+h_{wx}\omega_0+h_{wy}\dot{\phi}-h_{wy}\omega_0\psi\\&\quad-I_{yz}\ddot{\theta}+I_{xz}\ddot{\phi}-2I_{xy}\omega_0\dot{\theta}-I_{xz}\omega_0^2\phi-2I_{xz}\omega_0\dot{\psi}+I_{xy}\omega_0^2.\end{aligned}\tag{12}$$

3. Nonlinear gravity gradient moment equations

Gravity gradient torque plays a significant role in attitude control of satellites in LEO. Gravity gradient stabilization uses the earth's gravitational field to keep the spacecraft aligned in a nadir-looking orientation. The GG moments are modeled and explained in this section.

Gravity gradient moment is inherent in LEO satellites and cannot be neglected when dealing with passively-controlled spacecraft. Based on Newton's universal law of gravitation, the force in a gravity field is [1]:

$$d\mathbf{F}=-\frac{\mu dm}{\|\mathbf{r}\|^3}\times\mathbf{r}.\tag{13}$$

In Fig. 2, dm is mass element of the body in orbit, $\mathbf{r}$ is the distance of the mass element to CM of the earth, $\mathbf{R}$ is the distance of CM of the earth to CM of the moving satellite and $\boldsymbol{\rho}$ shows position of mass element relative to CM of satellite. Assuming a circular orbit, R_I in the inertial frame is presented by Eq. (14)

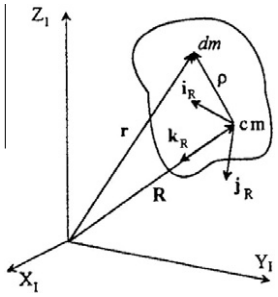

Fig. 2. The position of the CM in reference and inertial frames.

$$R_I = \begin{bmatrix} 0 \\ 0 \\ -R \end{bmatrix}. \tag{14}$$

R_I is transformed to the body frame using transformation matrix (C), given in Eq. (6)

$$R_B = CR_I. \tag{15}$$

$\mathbf{R}$ in body frame R_B is given by Eq. (16)

$$R_B = \begin{bmatrix} R\sin\theta \\ -R\sin\phi\cos\theta \\ -R\cos\phi\cos\theta \end{bmatrix}. \tag{16}$$

For the mass element, moment about CM of the body (dT_{GG}) comes from Eq. (17)

$$d\boldsymbol{T}_{GG} = \boldsymbol{\rho} \times d\boldsymbol{F} = -\frac{\mu dm}{|r|^3}\boldsymbol{\rho} \times \boldsymbol{r}. \tag{17}$$

Assuming $\rho \ll R_0, \frac{1}{|r|^3}$ is simplified and then total moment ($\boldsymbol{T}_{GG}$) is presented in Eq. (18)

$$\boldsymbol{T}_{GG} = -\frac{\mu}{R^3}\int\left(1 - \frac{3(\boldsymbol{R}.\boldsymbol{\rho})}{R^2}\right)(\boldsymbol{\rho} \times \boldsymbol{r})\,dm. \tag{18}$$

Considering algebraic relations and defining moments of inertia as $I_{xx} = \int(y^2 + z^2)\,dm, I_{yy} = \int(x^2 + z^2)\,dm, I_{zz} = \int(x^2 + y^2)\,dm$, and products of inertia as $I_{xy} = \int(xy)\,dm, I_{xz} = \int(xz)\,dm, I_{yz} = \int(yz)\,dm$, nonlinear model of the earth gravity gradient moment is obtained in roll, pitch and yaw axes as Eq. (19)

$$\begin{aligned}
G_x &= \frac{3\mu}{2R^3}\left[-(\cos\phi\sin 2\theta)I_{xy} + (\sin\phi\sin 2\theta)I_{xz} - 2(\cos^2\theta\cos 2\phi)I_{yz} + (\sin 2\phi\cos^2\theta)(I_z - I_y)\right], \\
G_y &= \frac{3\mu}{2R^3}\left[-(\sin\phi\sin 2\theta)I_{yz} - (\sin 2\phi\cos^2\theta)I_{xy} + 2(\sin^2\theta - \cos^2\phi\cos^2\theta)I_{xz} - (\cos\phi\sin 2\theta)(I_x - I_z)\right], \\
G_z &= \frac{3\mu}{2R^3}\left[(\sin 2\phi\cos^2\theta)I_{xz} + (\cos\phi\sin 2\theta)I_{yz} + 2(\sin^2\phi\cos^2\theta - \sin^2\theta)I_{xy} - (\sin\phi\sin 2\theta)(I_y - I_x)\right].
\end{aligned} \tag{19}$$

3.1. Gravity gradient moments linearization

In order to linearize GG moments, small angle assumption is applied. Therefore, values of cosine and sine are approximated by 1 and the value of angles in radians, respectively. By neglecting second order and higher terms, explained in Section 2.1, the linear gravity gradient moments approximation is obtained in Eq. (20)

$$\begin{aligned}
G_x &= 3\omega_o^2\left[-\theta I_{xy} - \phi I_{yz} + \phi(I_z - I_y)\right], \\
G_y &= 3\omega_o^2\left[-\phi I_{xy} - I_{xz} - \theta(I_x - I_z)\right], \\
G_z &= 3\omega_o^2\left[\phi I_{xz} + \theta I_{yz}\right].
\end{aligned} \tag{20}$$

3.2. Pure gravity gradient stabilization discussion

Gravity gradient moments are employed for pure passive stabilization [9]. Stability conditions cannot be studied in nonlinear model. Thus, linear attitude dynamics equations are used for the purpose of stability analysis. It is assumed that the system is passively controlled. Thus, control and disturbance torques and also momentum exchange devices terms are neglected. So Eq. (12) are rewritten in Eq. (21)

$$\begin{aligned}
&I_x\ddot{\phi} + 4\omega_0^2(I_y - I_z)\phi - \omega_0(I_x + I_z - I_y)\dot{\psi} = 0, \\
&I_y\ddot{\theta} + 3\omega_0^2(I_x - I_z)\theta = 0, \\
&I_z\ddot{\psi} + \omega_0^2(I_y - I_x)\psi + \omega_0(I_z + I_x - I_y)\dot{\phi} = 0.
\end{aligned} \tag{21}$$

Note that in Eqs. (21), I_x, I_y *and* I_z are defined in principal axes. Utilizing Laplace transform and characteristic equation for the motion about x_B, y_B and z_B-axes, two stable regions are found. For the first region, the stability conditions are: $I_y > I_x > I_z$ and

$I_y < I_x + I_z$, and for the second one: $I_x > I_z > I_y$ and $I_x < I_y + I_z$. Therefore, any spacecraft that satisfies one of these two conditions is GG purely passive stable [9].

4. Simulations

In the previous sections, nonlinear and linear attitude dynamics equations and gravity gradient moments were explained. Also, conditions for pure GG stabilization were given. In this section, the preceding theoretical results are supported through numerical simulations for illustrative examples. At first, for a specific satellite, attitude dynamics equations in the linear and nonlinear models are compared. According to an acceptable accuracy, the validity of linear approximation is determined in terms of the divergence of linear equation relative to the nonlinear model. Furthermore, based on utilizing or neglecting GG moments in attitude dynamics equations, weights of these moments are illustrated. Then, the nonlinear and linear equations of gravity gradient moments are simulated and error of the linear approximation is discussed. In the last subsection, the analytical solution is compared with the numerical one.

4.1. Attitude dynamics equation simulation

The selected spacecraft moments of inertia satisfy pure GG stabilization condition (see Section 3.2). The satellite mission was designed for LEO at an altitude of 500 km. Tensor of inertia and orbital period are as:

$$I = \begin{bmatrix} 6 & 0 & 0 \\ 0 & 8 & 0 \\ 0 & 0 & 4 \end{bmatrix},$$

$$\textit{orbital period} = \frac{2\pi}{\omega_0} = 94.47 \text{ min}.$$

4.1.1. Utilizing GG moments

Figs. 3–8 show attitude angles behavior utilizing nonlinear and linear spacecraft attitude equations in 1.6 times orbital periods. The initial attitude angles are increased from 1° to 25° in intervals of 5°. Divergence of linear equation is clearly shown in Figs. 3–8. Notice that in these simulations gravity gradient effects are considered.

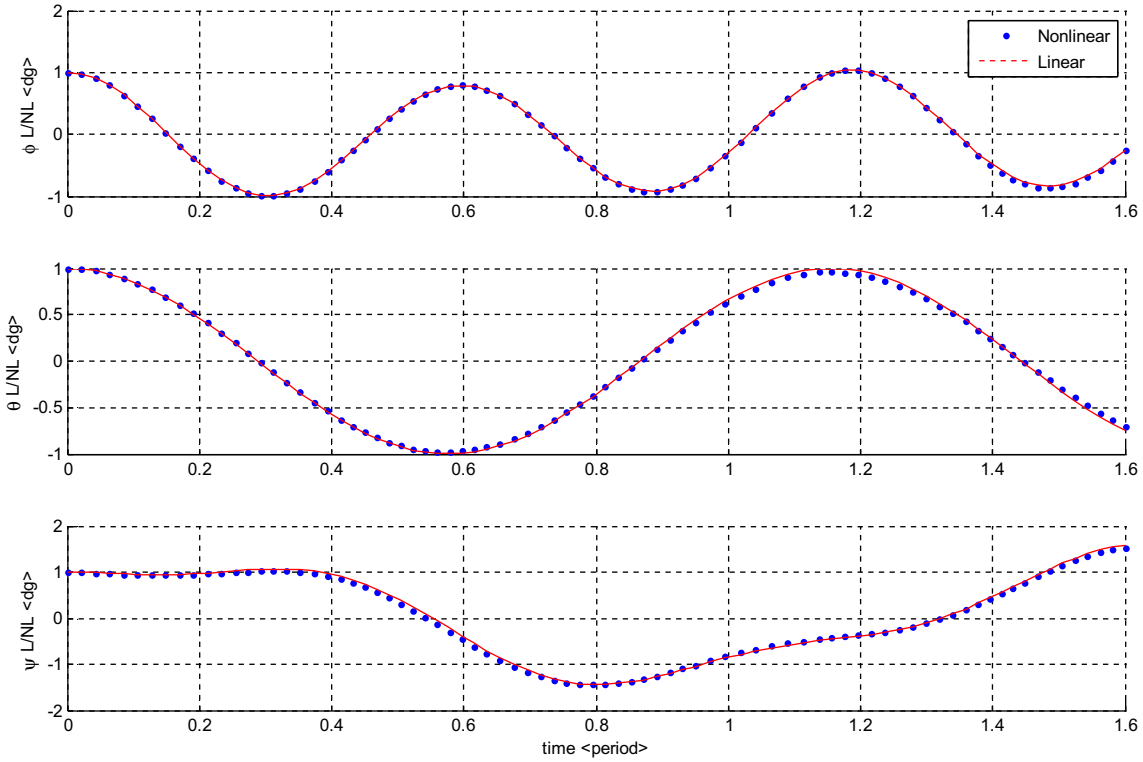

Fig. 3. Attitude angles history, utilizing GG moments, with 1° initial condition on roll, pitch and yaw.

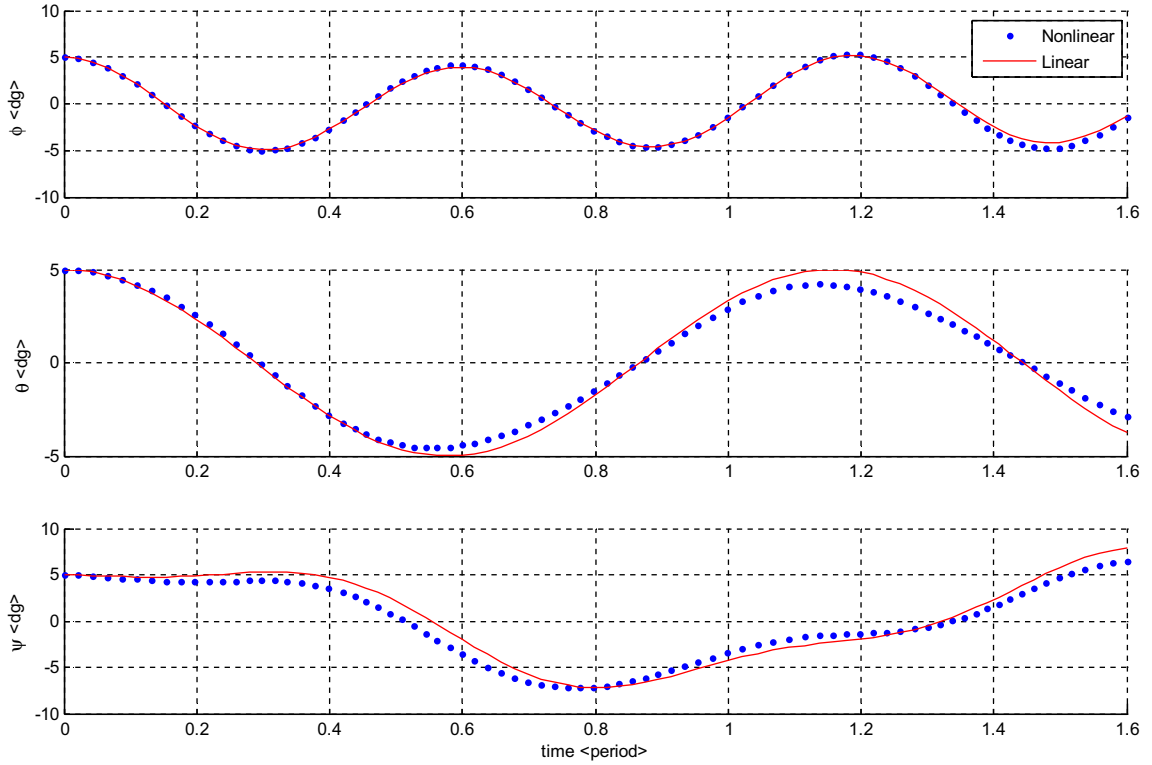

Fig. 4. Attitude angles history, utilizing GG moments, with 5° initial condition on roll, pitch and yaw.

Eqs. (22) are used to calculate error of the linear approximation

$$\begin{aligned} &Error_i = e_i = \frac{|Euler_{linear} - Euler_{nonlinear}|}{|Euler_{nonlinear}|} \times 100, \quad i = 1, \ldots, N, \\ &Error\ of\ Euler = E_{Euler} = \frac{e_1 + e_2 + e_3 + \cdots + e_N}{N}, \quad Euler = \phi, \theta, \psi, \\ &Mean\ of\ E_{Euler} = ME = \frac{E_{roll} + E_{pitch} + E_{yaw}}{3}. \end{aligned} \tag{22}$$

Fig. 9 shows mean error percentage as a function of attitude angles.

Table 1 presents numerical results of error percentage on each roll, pitch and yaw axes and their respective mean values.

4.1.2. Neglecting GG moments

Study of this case is similar to the previous one but here gravity gradient moments are neglected. Figs. 10–16 show attitude angles behavior utilizing nonlinear and linear attitude equations in 1.6 times orbital periods, for increasing attitude angles. Divergence of linear equations is presented in Figs. 10–16.

Utilizing Eqs. (22), Fig. 16 shows mean error percentage regarding increase in attitude angles.

Table 2 presents numerical results of error percentage on each roll, pitch and yaw axes and their respective mean values.

4.2. Linear and nonlinear gravity gradient comparison

In order to find linearization error of gravity gradient moments, numerical simulations are carried for the case: $I_x = 6$, $I_y = 8$, $I_z = 4$, $R = R_E + 500$ km and $R_E = 6378.137$ km (equatorial radius of the earth). Fig. 17 shows gravity gradient moment components in linear and nonlinear models.

Eqs. (23) are used to calculate error of linear approximation of GG moments. In developing Eqs. (23) linearization error on yaw axis (E_{GG_z}) is excluded since linear model of GG moment on yaw axis is not a function of principal moments of inertia

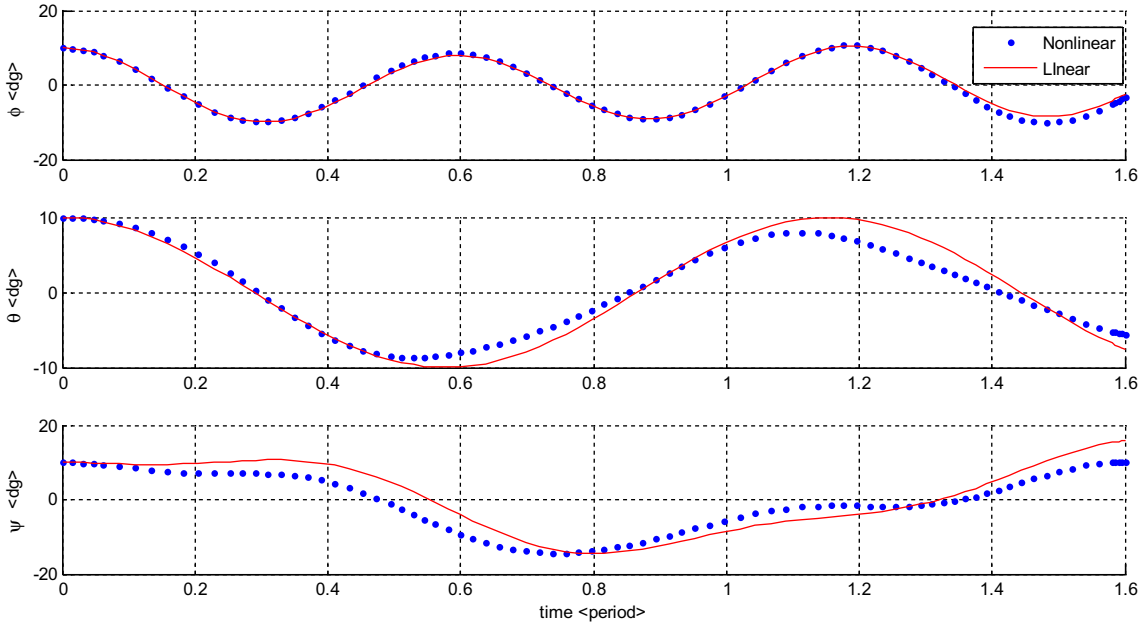

Fig. 5. Attitude angles history, utilizing GG moments, with 10° initial condition on roll, pitch and yaw.

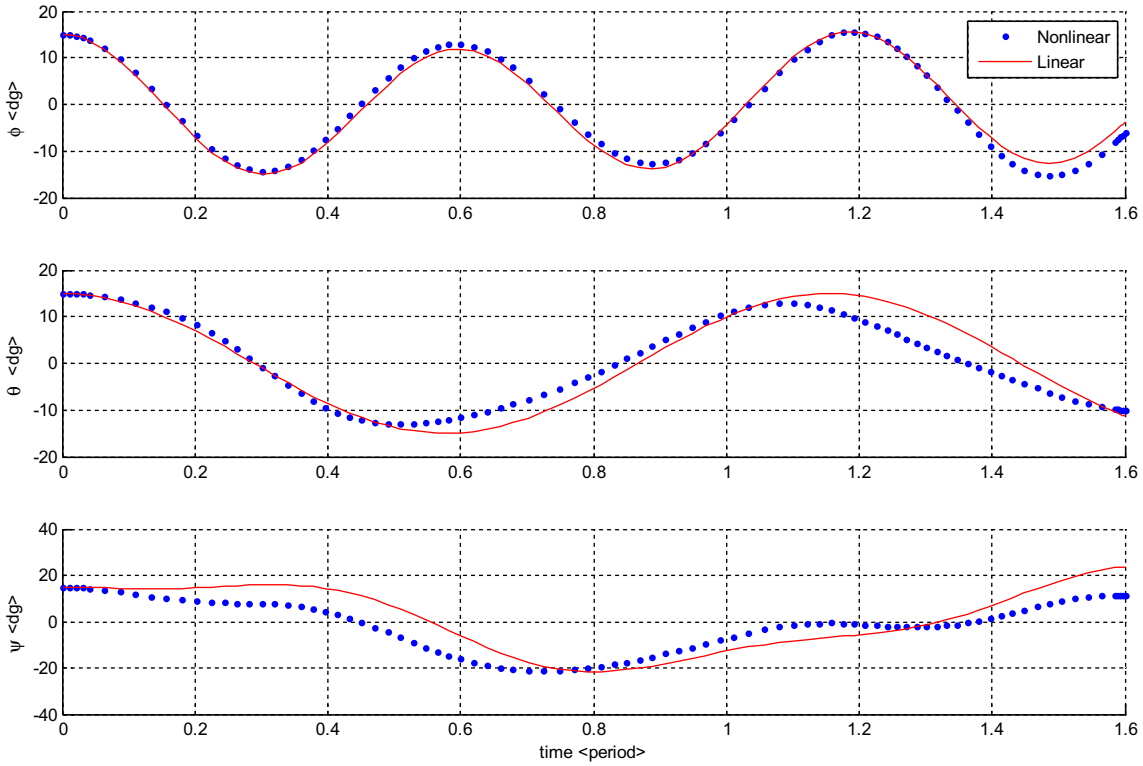

Fig. 6. Attitude angles history, utilizing GG moments, with 15° initial condition on roll, pitch and yaw.

(Eq. (20)). Thus in our case study dealing with the principal axes, relative error on yaw axis is equal to 100% for the all attitude angles and is neglected in calculating mean error

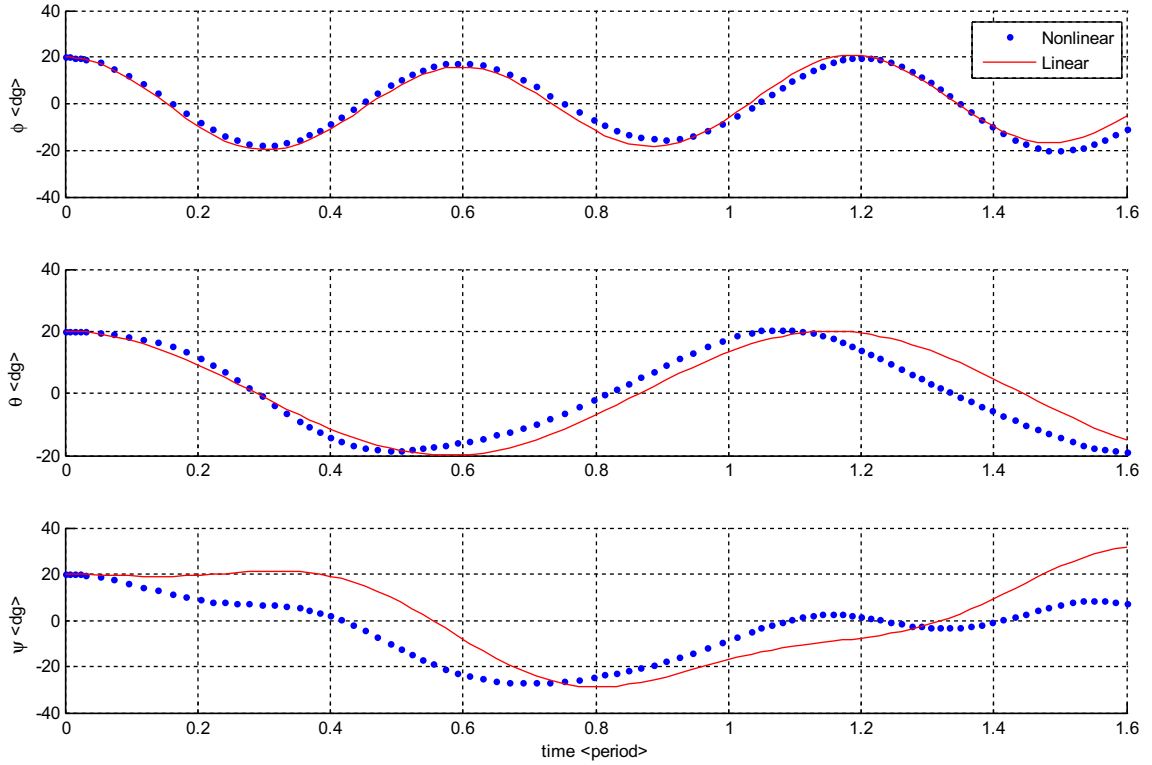

Fig. 7. Attitude angles history, utilizing GG moments, with 20° initial condition on roll, pitch and yaw.

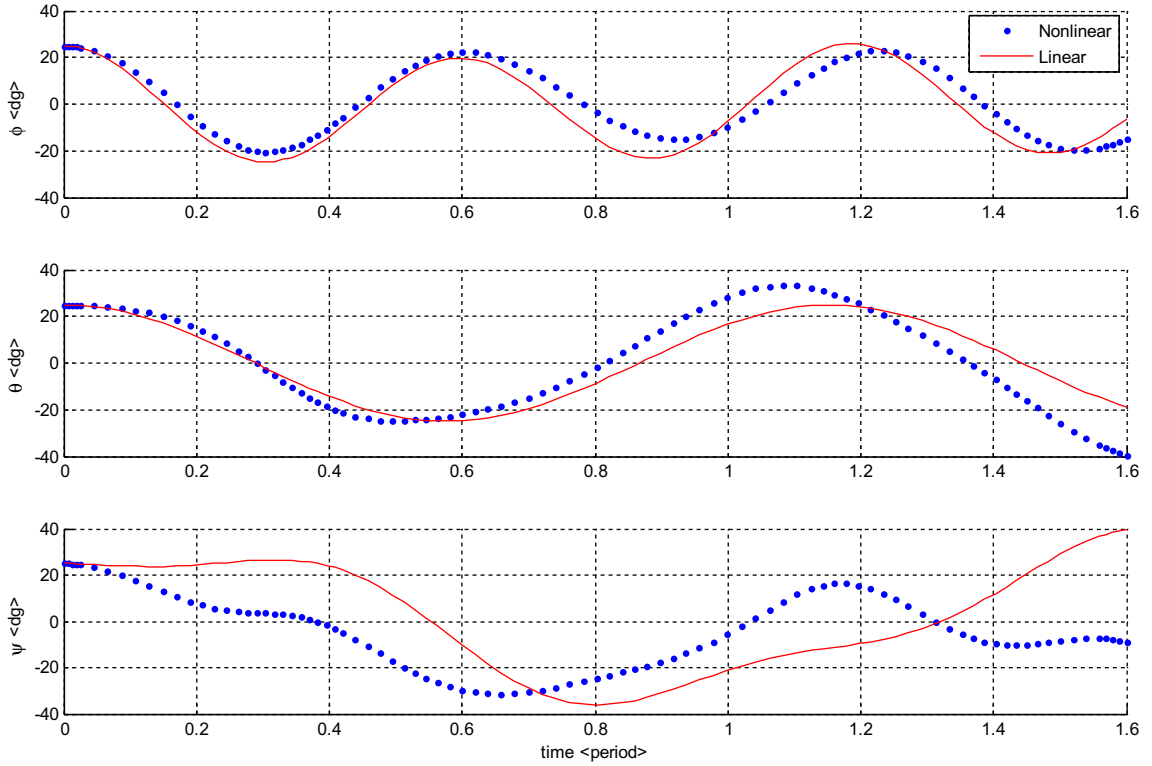

Fig. 8. Attitude angles history, utilizing GG moments, with 25° initial condition on roll, pitch and yaw.

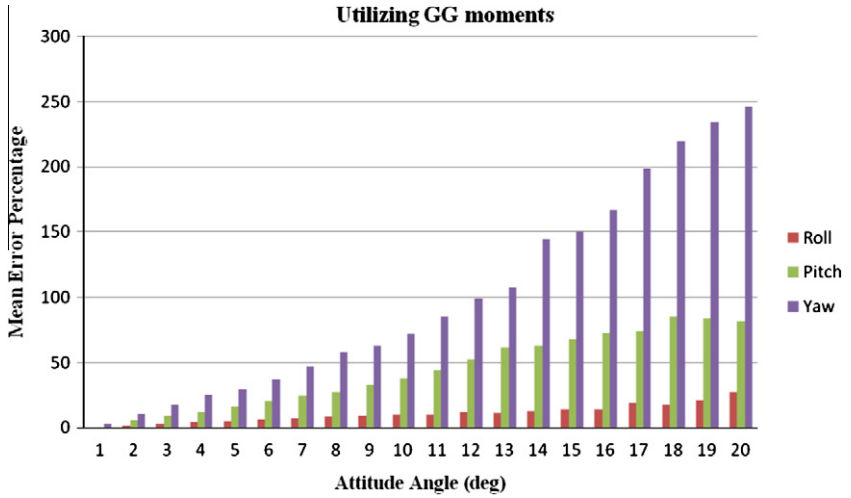

Fig. 9. Mean error percentage of linear approximation versus increasing attitude angles, utilizing GG moments.

Table 1
Mean error percentage of linear approximation, utilizing GG moments.

Attitude angles (°)	E_ϕ	E_θ	E_ψ	ME
1	0.19	0	2.64	0.94
2	1.65	5.92	10.29	5.95
3	3.00	9.01	17.36	9.79
4	4.34	12.17	24.81	13.77
5	5.37	15.90	29.56	16.94
6	6.43	20.08	37.00	21.17
7	7.41	24.24	46.43	26.03
8	8.74	26.98	57.89	31.20
9	9.12	32.81	62.93	34.95
10	9.70	37.65	71.93	39.76
11	10.24	43.75	85.00	46.33
12	12.00	52.50	99.35	54.62
13	11.10	61.41	107.10	59.87
14	13.02	62.70	144.30	73.34
15	13.80	67.73	149.79	77.11
16	14.24	72.90	166.42	84.52
17	19.02	74.02	198.94	97.33
18	17.44	85.19	220.01	107.55
19	21.06	83.57	234.29	112.97
20	27.60	81.88	246.33	118.60

$$E_{GG} = \frac{|GG_{linear} - GG_{nonlinear}|}{|GG_{nonlinear}|} \times 100,$$
$$ME_{GG} = \frac{E_{GG_x} + E_{GG_y}}{2}. \tag{23}$$

Considering Eqs. (23), Fig. 18 shows mean error percentage for increasing attitude angles.

Table 3 presents error percentage of linearization on each roll, pitch and yaw axes and their mean values.

4.3. Analytical solution

In this part analytical results [1] are compared with the results of numerical simulation. The attitude motion equations (Eqs. (12)) considering gravity gradient moments and neglecting disturbance torques will be as follows [1].

$$I_x\ddot{\phi} + 4\omega_0^2(I_y - I_z)\phi - \omega_0(I_x + I_z - I_y)\dot{\psi} = 0,$$
$$I_y\ddot{\theta} + 3\omega_0^2(I_x - I_z)\theta = 0, \tag{24}$$
$$I_z\ddot{\psi} + \omega_0^2(I_y - I_x)\psi + \omega_0(I_z + I_x - I_y)\dot{\phi} = 0.$$

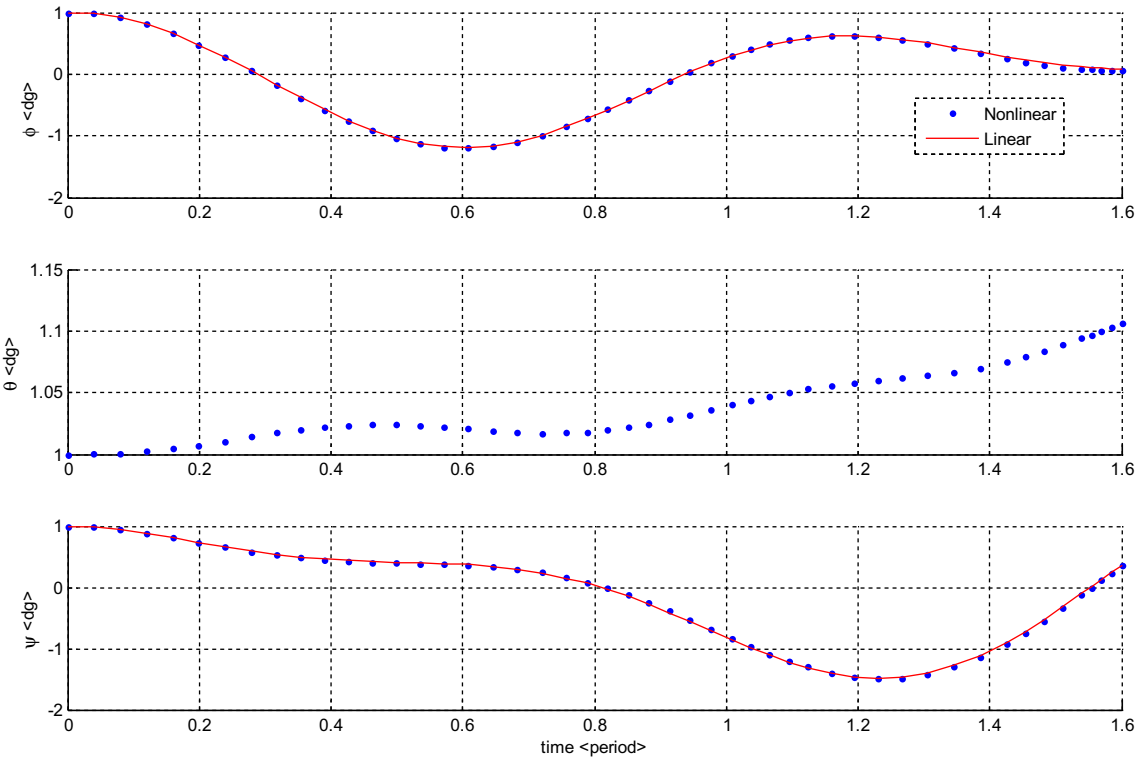

Fig. 10. Attitude angles history, neglecting GG moments, with 1° initial condition on roll, pitch and yaw.

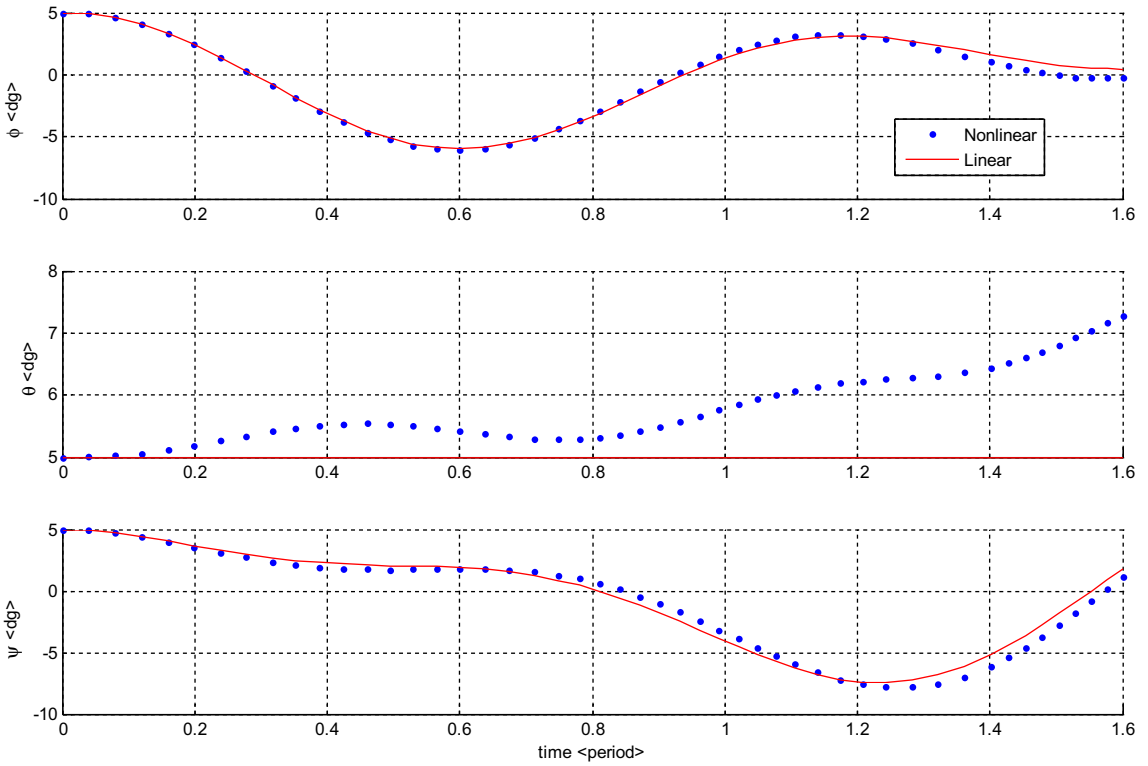

Fig. 11. Attitude angles history, neglecting GG moments, with 5° initial condition on roll, pitch and yaw.

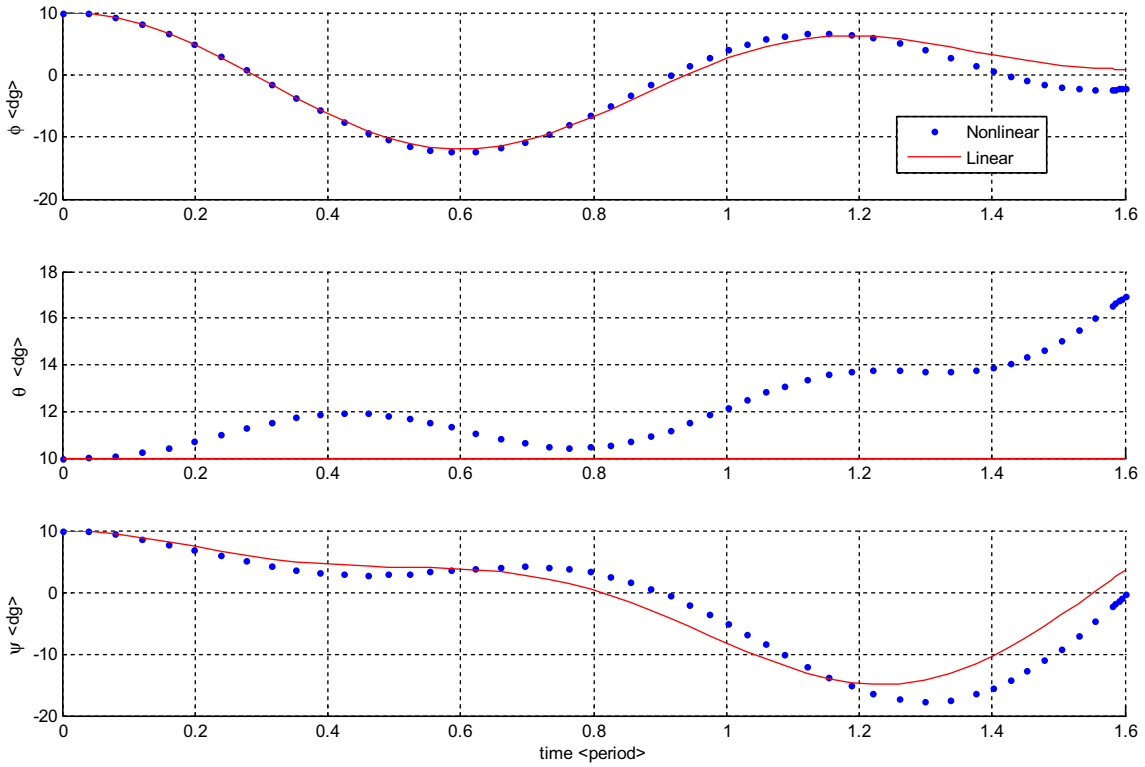

Fig. 12. Attitude angles, neglecting GG moments, with 10° initial condition on roll, pitch and yaw.

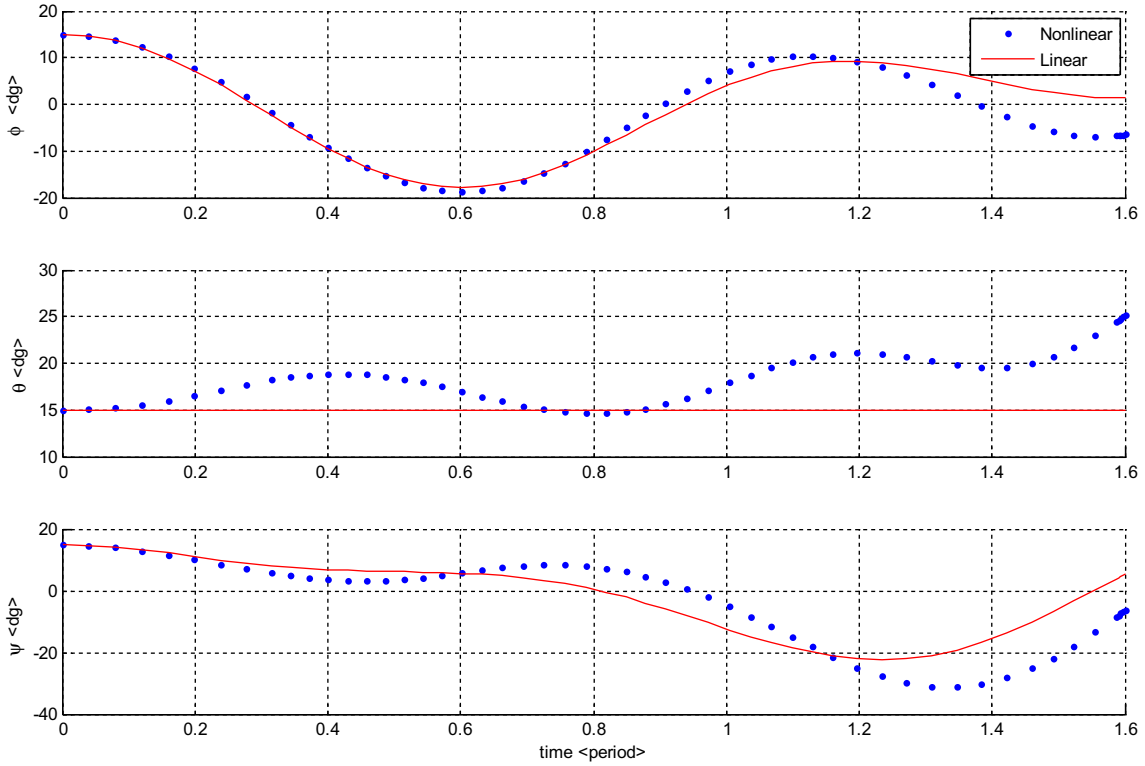

Fig. 13. Attitude angles, neglecting GG moments, with 15° initial condition on roll, pitch and yaw.

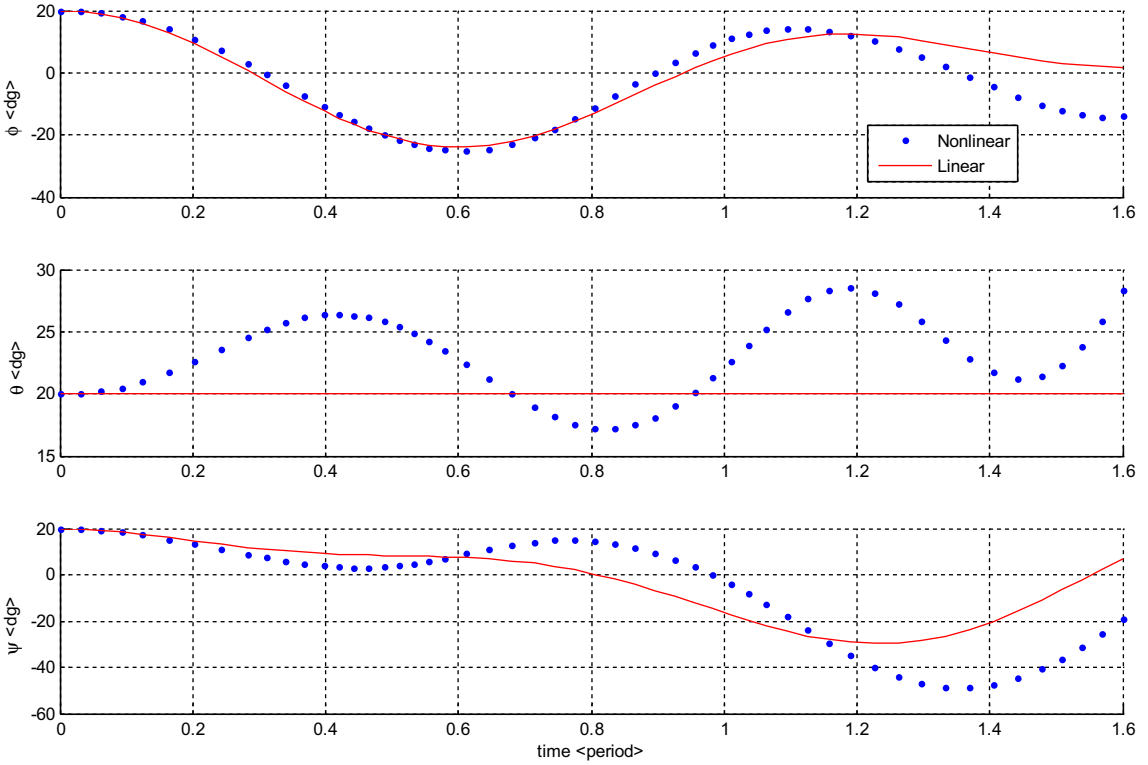

Fig. 14. Attitude angles, neglecting GG moments, with 20° initial condition on roll, pitch and yaw.

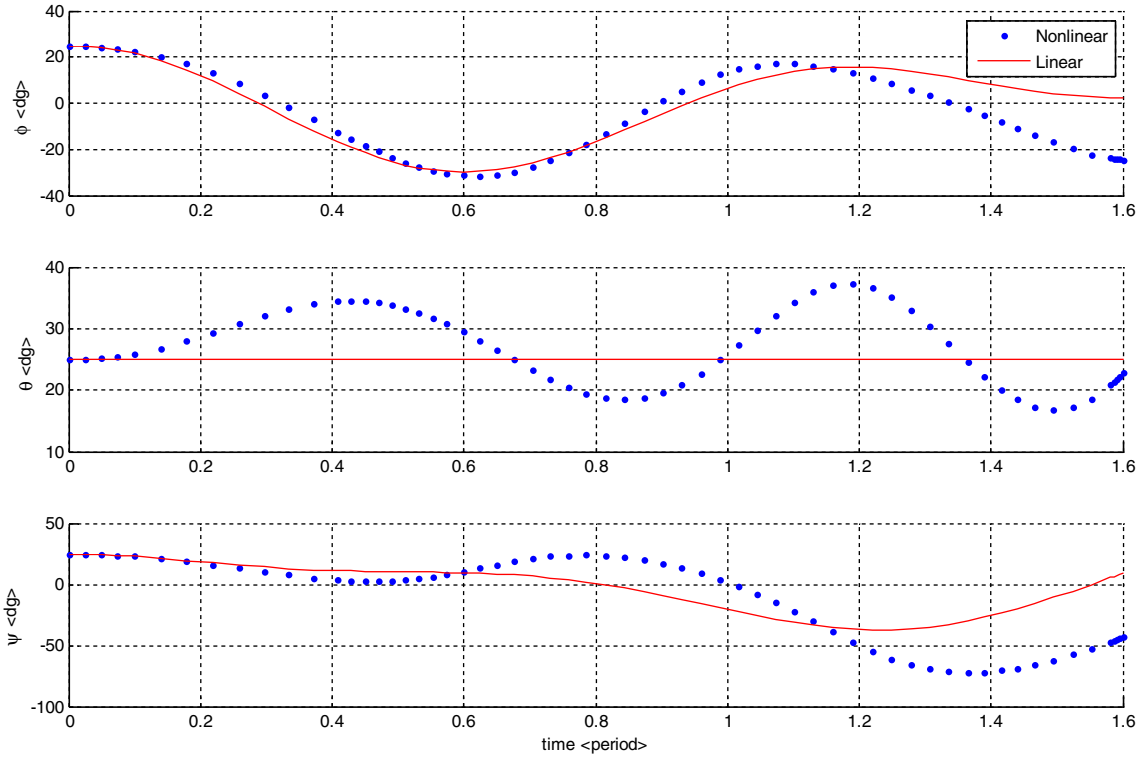

Fig. 15. Attitude angles, neglecting GG moments, with 25° initial condition on roll, pitch and yaw.

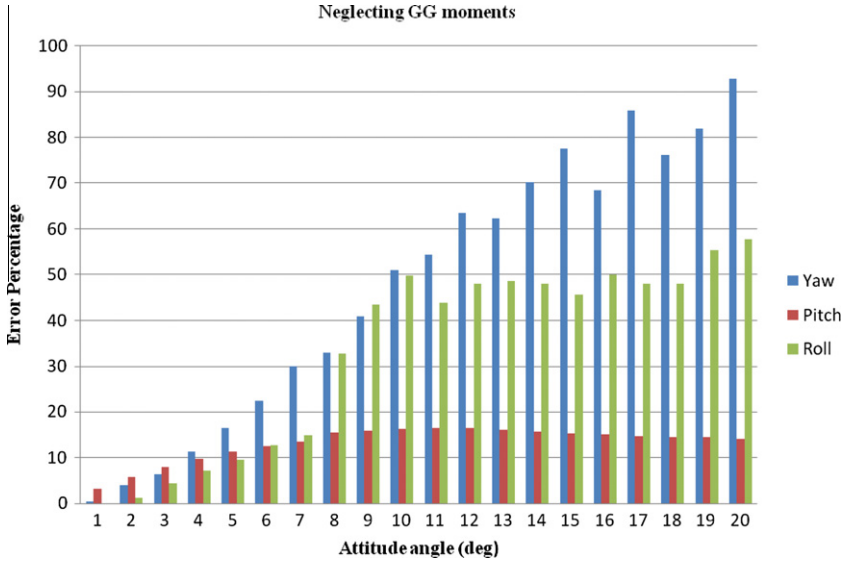

Fig. 16. Mean error of linear approximation for increasing attitude angles, neglecting GG moments.

Table 2
Mean error of linear approximation, neglecting GG moments.

Attitude angles (°)	E_ϕ	E_θ	E_ψ	ME
1	0.06	3.19	0.41	1.22
2	1.33	5.84	3.88	3.68
3	4.50	8.03	6.27	6.27
4	7.28	9.82	11.41	9.50
5	9.53	11.29	16.43	12.42
6	12.65	12.47	23.50	16.21
7	14.98	13.41	29.94	19.44
8	32.86	15.45	32.88	27.06
9	43.50	15.96	40.78	33.41
10	49.85	16.28	50.97	39.03
11	43.79	16.42	54.30	38.17
12	48.01	16.38	63.51	42.63
13	48.70	16.15	62.21	42.35
14	48.12	15.71	70.19	44.67
15	45.57	15.21	77.63	46.14
16	50.05	15.00	68.47	44.51
17	48.05	14.74	85.88	49.56
18	48.11	14.54	76.24	46.30
19	55.44	14.47	81.98	50.63
20	57.68	14.04	92.88	54.87

For the ease of notation we define:

$$\sigma_x = \frac{I_y - I_z}{I_x}, \quad \sigma_y = \frac{I_x - I_z}{I_y}, \quad \sigma_z = \frac{I_y - I_x}{I_z}. \tag{25}$$

As it can be seen pitch axis is independent from roll and yaw.

$$\begin{aligned} &I_y\ddot{\theta} + 3\omega_0^2(I_x - I_z)\theta = 0, \\ &\ddot{\theta} + 3\omega_0^2\sigma_y\theta = 0. \end{aligned} \tag{26}$$

Using Laplace transform, we have:

$$\begin{aligned} &s^2\Theta(s) - s\theta_0 - \dot{\theta}_0 + 3\omega_0^2\sigma_y\Theta(s) = 0, \\ &\Theta(s) = \frac{s\theta_0 + \dot{\theta}_0}{s^2 + 3\omega_0^2\sigma_y}, \\ &\Theta(s) = \theta_0\frac{s}{s^2 + 3\omega_0^2\sigma_y} + \dot{\theta}_0\frac{1}{s^2 + 3\omega_0^2\sigma_y}. \end{aligned} \tag{27}$$

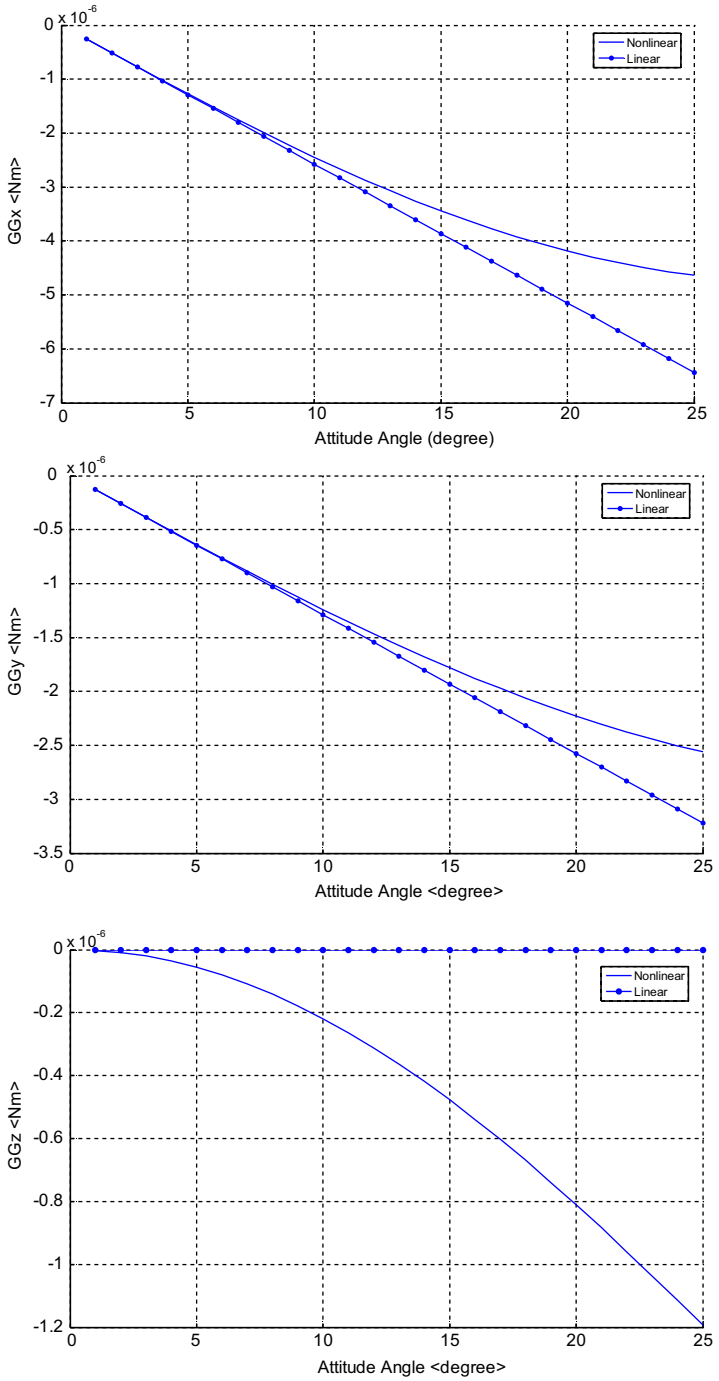

Fig. 17. Linear and nonlinear models of gravity gradient moment components as a function of attitude angle.

Time domain behavior about pitch axis is as Eq. (28).

$$\theta(t) = \theta_0 \cos\left(\sqrt{3\omega_0^2\sigma_y}t\right) + \frac{\dot{\theta}_0}{\sqrt{3\omega_0^2\sigma_y}} \sin\left(\sqrt{3\omega_0^2\sigma_y}t\right). \tag{28}$$

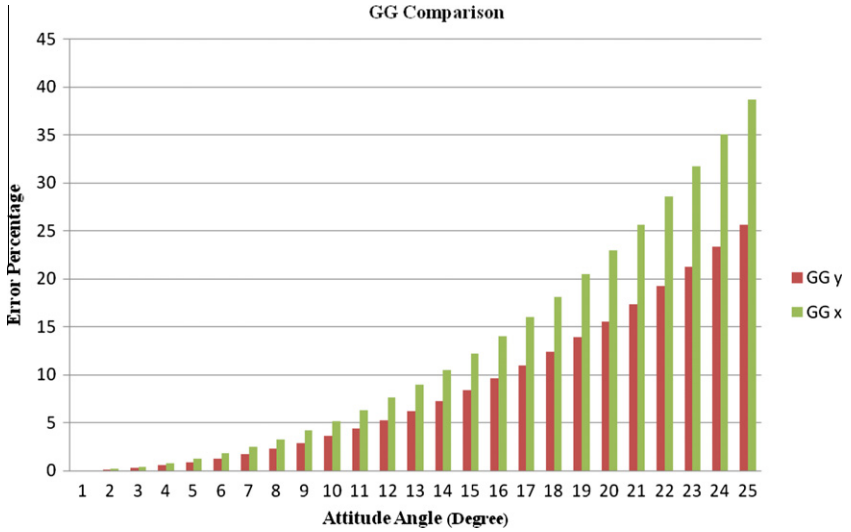

Fig. 18. Linearization error for gravity gradient moments for increasing attitude angles.

Taking Laplace transform leads to the following equations for roll and yaw axes [1]:

$$\begin{aligned}
&I_x\ddot{\phi} + 4\omega_0^2(I_y - I_z)\phi - \omega_0(I_x + I_z - I_y)\dot{\psi} = 0,\\
&\ddot{\phi} + 4\omega_0^2\sigma_x\phi - \omega_0(1-\sigma_x)\dot{\psi} = 0,\\
&s^2\Phi(s) - s\phi_0 - \dot{\phi}_0 + 4\omega_0^2\sigma_x\Phi(s) - \omega_0(1-\sigma_x)(s\Psi(s) - \psi_0) = 0,\\
&(s^2 + 4\omega_0^2\sigma_x)\Phi(s) - s\omega_0(1-\sigma_x)\Psi(s) = s\phi_0 + \dot{\phi}_0 - \omega_0(1-\sigma_x)\psi_0,\\
&I_z\ddot{\psi} + \omega_0^2(I_y - I_x)\psi + \omega_0(I_z + I_x - I_y)\dot{\phi} = 0,\\
&\ddot{\psi} + \omega_0^2\sigma_z\psi + \omega_0(1-\sigma_z)\dot{\phi} = 0,\\
&s^2\Psi(s) - s\psi_0 - \dot{\psi}_0 + \omega_0^2\sigma_z\Psi(s) + \omega_0(1-\sigma_z)(s\Phi(s) - \phi_0),\\
&(s^2 + \omega_0^2\sigma_z)\Psi(s) + s\omega_0(1-\sigma_z)\Phi(s) = s\psi_0 + \dot{\psi}_0 + \omega_0(1-\sigma_z)\phi_0.
\end{aligned} \tag{29}$$

As a result, one may write:

$$\begin{cases}
(s^2 + 4\omega_0^2\sigma_x)\Phi(s) - s\omega_0(1-\sigma_x)\Psi(s) = s\phi_0 + \dot{\phi}_0 - \omega_0(1-\sigma_x)\psi_0,\\
(s^2 + \omega_0^2\sigma_z)\Psi(s) + s\omega_0(1-\sigma_z)\Phi(s) = s\psi_0 + \dot{\psi}_0 + \omega_0(1-\sigma_z)\phi_0.
\end{cases} \tag{30}$$

The analytical solution utilizing Laplace transform is only available in some cases. Here we assume $\dot{\phi}_0, \dot{\psi}_0 = 0$ and the system for $\Phi(s)$ and $\Psi(s)$ will be as follows:

$$\begin{aligned}
\Phi(s) &= \frac{s^3\phi_0 + s\omega_0^2\phi_0(1 - \sigma_x + \sigma_x\sigma_z) + \omega_0^3\sigma_z\psi_0(\sigma_x - 1)}{s^4 + s^2\omega_0^2(3\sigma_x + 1 + \sigma_x\sigma_z) + 4\omega_0^4\sigma_x\sigma_z},\\
\Psi(s) &= \frac{s^3\psi_0 + s\omega_0^2\psi_0(1 + 3\sigma_x + \sigma_x\sigma_z - \sigma_z) + 4\omega_0^3\sigma_x\phi_0(1-\sigma_z)}{s^4 + s^2\omega_0^2(3\sigma_x + 1 + \sigma_x\sigma_z) + 4\omega_0^4\sigma_x\sigma_z}.
\end{aligned} \tag{31}$$

The denominator is rewritten as Eq. (32)

$$s^4 + s^2\omega_0^2(3\sigma_x + 1 + \sigma_x\sigma_z) + 4\omega_0^4\sigma_x\sigma_z \equiv s^4 + s^2\left(\omega_1^2 + \omega_2^2\right) + \omega_1^2\omega_2^2 = \left(s^2 + \omega_1^2\right)\left(s^2 + \omega_2^2\right), \tag{32}$$

So

$$\begin{cases}
\omega_0^2(3\sigma_x + 1 + \sigma_x\sigma_z) = \frac{10}{3}\omega_0^2 \equiv \omega_1^2 + \omega_2^2\\
4\omega_0^4\sigma_x\sigma_z = \frac{4}{3}\omega_0^4 \equiv \omega_1^2\omega_2^2
\end{cases}, \quad \rightarrow \begin{cases}
\omega_1^2 + \omega_2^2 = \frac{10}{3}\omega_0^2\\
\omega_1^2\omega_2^2 = \frac{4}{3}\omega_0^4
\end{cases}, \quad \rightarrow \quad \omega_1^2 = 2.8685\omega_0^2, \omega_2^2 = 0.4648\omega_0^2. \tag{33}$$

Assuming $\phi_0 = 0$, the system is solved as Eqs. (34) and (35). It should be mentioned that these assumptions are necessary to utilize analytical solution.

Table 3
The linearization error percentage.

Attitude angles (°)	E_{GG_x}	E_{GG_y}	ME_{GG}	E_{GG_z}
1	0.05	0.04	0.045	100
2	0.20	0.14	0.17	100
3	0.46	0.32	0.39	100
4	0.82	0.57	0.695	100
5	1.28	0.89	1.085	100
6	1.85	1.29	1.57	100
7	2.53	1.76	2.145	100
8	3.31	2.31	2.81	100
9	4.21	2.93	3.57	100
10	5.23	3.63	4.43	100
11	6.37	4.42	5.395	100
12	7.63	5.29	6.46	100
13	9.03	6.24	7.635	100
14	10.57	7.28	8.925	100
15	12.23	8.41	10.32	100
16	14.06	9.64	11.85	100
17	16.04	10.97	13.505	100
18	18.18	12.40	15.29	100
19	20.50	13.93	17.215	100
20	23.00	15.58	19.29	100
21	25.69	17.34	21.515	100
22	28.60	19.23	23.915	100
23	31.72	21.25	26.485	100
24	35.08	23.4	29.24	100
25	38.69	25.69	32.19	100

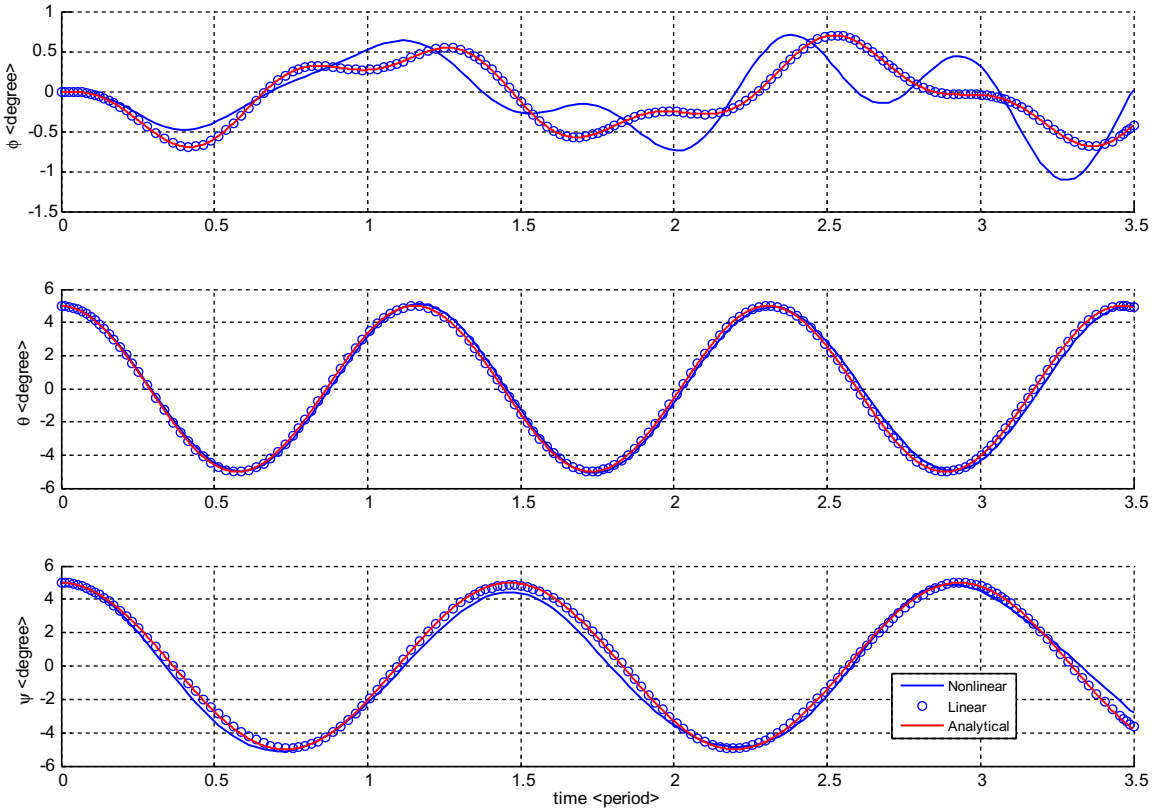

Fig. 19. The results of analytical solution in comparison with the linear and nonlinear numerical simulation for $\phi_0 = 0°$, $\theta_0 = 5°$,$\psi_0 = 5°$.

$$\begin{aligned}\Phi(s) &= \frac{\omega_0^3\sigma_z\psi_0(\sigma_x-1)}{s^4+s^2\omega_0^2(3\sigma_x+1+\sigma_x\sigma_z)+4\omega_0^4\sigma_x\sigma_z},\\ &= \omega_0^3\sigma_z\psi_0(\sigma_x-1)\frac{1}{(s^2+\omega_1^2)(s^2+\omega_2^2)}, \quad A=\frac{-1}{\omega_2^2-\omega_1^2},\\ \Phi(s) &= \omega_0^3\sigma_z\psi_0(\sigma_x-1)\frac{1}{(s^2+\omega_1^2)(s^2+\omega_2^2)},\\ &= \omega_0^3\sigma_z\psi_0(\sigma_x-1)\left(\frac{A}{\omega_1}.\frac{\omega_1}{s^2+\omega_1^2}-\frac{A}{\omega_2}.\frac{\omega_2}{s^2+\omega_2^2}\right),\end{aligned} \tag{34}$$

$$\begin{aligned}\Psi(s) &= \frac{s^3\psi_0+s\omega_0^2\psi_0(1+3\sigma_x+\sigma_x\sigma_z-\sigma_z)}{s^4+s^2\omega_0^2(1+3\sigma_x+1+\sigma_x\sigma_z)+4\omega_0^4\sigma_x\sigma_z}=\frac{\psi_0 s(s^2+\omega_0^2(1+3\sigma_x+\sigma_x\sigma_z-\sigma_z))}{s^4+s^2\omega_0^2(1+3\sigma_x+1+\sigma_x\sigma_z)+4\omega_0^4\sigma_x\sigma_z}\\ &= \frac{\psi_0 s(s^2+\omega_0^2(1+3\sigma_x+\sigma_x\sigma_z-\sigma_z))}{(s^2+\omega_1^2)(s^2+\omega_2^2)}.\end{aligned} \tag{35}$$

Time domain behavior of roll axis is obtained as follows:

$$\begin{aligned}\Phi(s) &= \omega_0^3\sigma_z\psi_0(\sigma_x-1)\left(\frac{A}{\omega_1}.\frac{\omega_1}{s^2+\omega_1^2}-\frac{A}{\omega_2}.\frac{\omega_2}{s^2+\omega_2^2}\right),\\ \phi(t) &= \omega_0^3\sigma_z(\sigma_x-1)A\left(\frac{\sin(\omega_1 t)}{\omega_1}-\frac{\sin(\omega_2 t)}{\omega_2}\right)\psi_0,\end{aligned} \tag{36}$$

and for yaw axis is:

$$\Psi(s) = \frac{\psi_0 s(s^2+\omega_0^2(1+3\sigma_x+\sigma_x\sigma_z-\sigma_z))}{(s^2+\omega_1^2)(s^2+\omega_2^2)}. \tag{37}$$

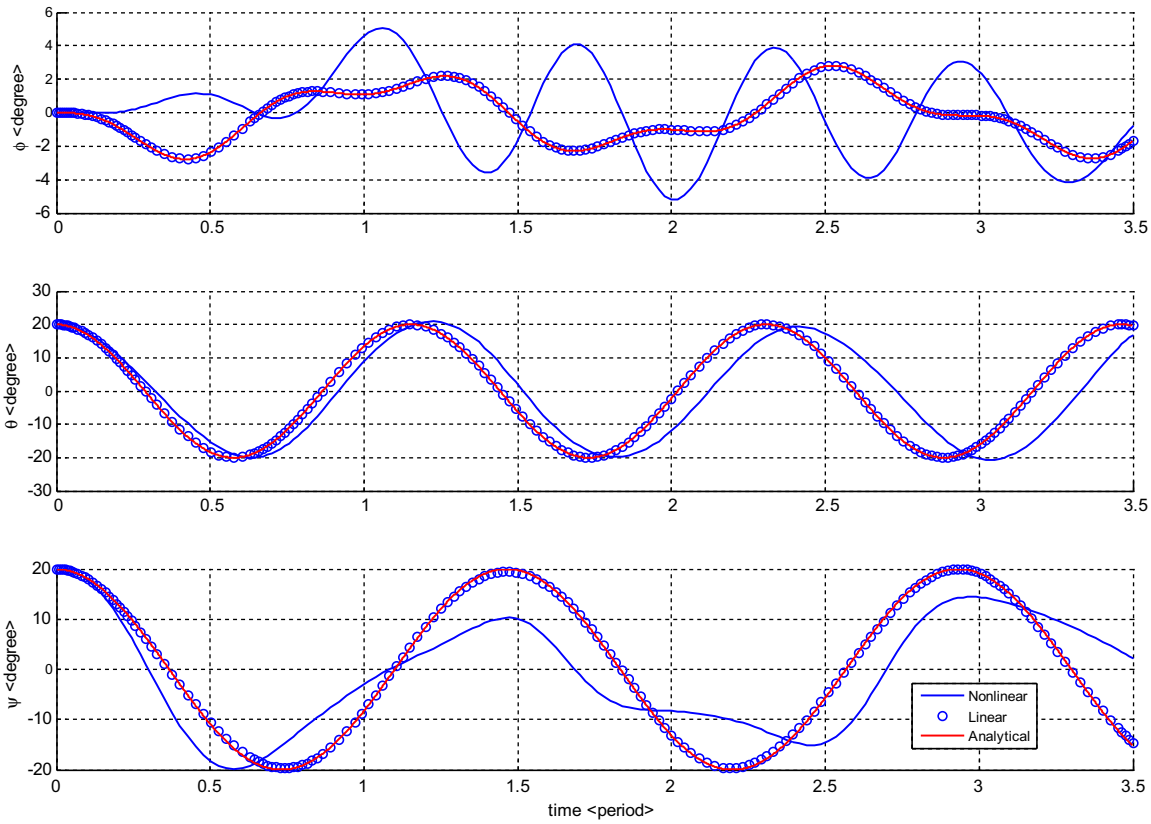

Fig. 20. The results of analytical solution in comparison with the linear and nonlinear numerical simulation for $\phi_0 = 0°$, $\theta_0 = 20°$, $\psi_0 = 20°$.

Numerical values are employed in order to utilize inverse Laplace method.

$$I_x = 6, \quad I_y = 8, \quad I_z = 6 \rightarrow \omega_o = 0.0011, \quad \sigma_x = 0.6667, \quad \sigma_y = 0.2500, \quad \sigma_z = 0.5000,$$
$$\omega_1 = 1.6937\omega_0, \quad \omega_2 = 1.6937\omega_0, \quad \omega_o = 0.0011,$$

$$\Psi(s) = \frac{\psi_0 s\left(s^2 + \omega_0^2(1 + 3\sigma_x + \sigma_x\sigma_z - \sigma_z)\right)}{\left(s^2 + \omega_1^2\right)\left(s^2 + \omega_2^2\right)} = \frac{\psi_0 s(s^2 + 3.4816 \times 10^{-6})}{(s^2 + 3.5249 \times 10^{-6})(s^2 + 5.7120 \times 10^{-6})} \simeq \frac{\psi_0 s}{(s^2 + 5.7120 \times 10^{-6})}$$
$$= \psi_0 \frac{s}{\left(s^2 + \omega_2^2\right)}. \tag{38}$$

So for time domain behavior on yaw axis we have Eq. (39)

$$\psi(t) = \psi_0 \cos(\omega_2 t). \tag{39}$$

Figs. 19 and 20 show results of analytical solution in comparison with linear and nonlinear numerical simulation. As it can be seen, analytical solution closely follows the linear numerical solution. However, it can only be used in few and limited cases.

5. Discussion

In this study, nonlinear and linear models of spacecraft attitude equations and gravity gradient moments are simulated. Figs. 3–8 and Figs. 10–15 show divergence of linear approximation of attitude equations compared to the nonlinear model. Figs. 9 and 16 show that increasing the attitude angle raises linearization error. According to the desired accuracy, it is possible to introduce the upper bound for "small angle" assumed in linearization. For instance, according to Fig. 9 if acceptable error percentage is equal to 10, upper bound for the small angle linearization is 3°. In the next simulation, neglecting GG moments, upper bound of small attitude angle is 4°, assuming a desired error percentage of 10. Therefore in this example, linear approximation is not valid for attitude angles larger than 4°.

A comparison between Figs. 9 and 16 indicates that considering GG moments as external torque for large attitude angles such as 20° amplifies error percentage more than twice. In addition, Fig. 9 is smoother than Fig. 16 due to the influence of gravity gradient torques. Fig. 18 shows a raising tendency of linearization error of GG moments as a function of increasing attitude angles. For yaw axis, linearization error percentage equals 100 because linear GG moment on this axis is equal to zero. For initial conditions equal to 25°, error percentages are about 38 and 25 on roll and pitch axes, respectively. Neglecting the yaw error, for 10% linearization error, the upper bound for "small angle" assumption for attitude angles is 15°. In the last part, analytical solution is compared with the numerical one and results show that analytical and linear solutions lead to similar plots. It should be mentioned that analytical solution is available only in limited cases with simplifying assumptions. We apply analytical solution in order to validate linear simulation. According to the above mentioned results, it is possible to find the linearization error for different attitude angles and then to introduce a criterion for defining the upper bound for valid assumption of "small angle".

6. Conclusion

The purpose of this paper is to compare the nonlinear and linear models of the spacecraft attitude dynamics and the gravity gradient moments in order to determine divergence of linear approximation relative to the nonlinear model. Simulations show that divergence of linear approximation relative to nonlinear model grows by increasing attitude angles. It is noticeable that using gravity gradient moments increases the linearization error. Moreover, gravity gradient influence should be considered as an important factor especially in low earth orbits. According to spacecraft attitude dynamics equations, error tendency depends on the tensor of inertia and altitude of the satellite. Therefore, for any specific case, designer of spacecraft attitude control subsystem should investigate validity of linear model based on desired mission accuracy. In addition, gravity gradient moments simulations show that divergence of linear model has a raising tendency as a function of increasing attitude angles. It indicates that using linear or nonlinear models of GG torques especially in low earth orbits should be chosen very cautiously. In this way it is possible to define the upper bound of small angle for any specific satellite based on desired accuracy of the mission which keeps the linear model valid and applicable.

Acknowledgment

Authors would like to thank the three referees for carefully reading this paper and for their comments and suggestions which have improved the paper significantly.

References

[1] Sidi Marcel. Spacecraft dynamics and control, a practical engineering approach. Cambridge University Press; 2003.
[2] Stevens Brian L, Lewis Frank L. Aircraft control and simulation. Wiley-IEEE; 2003.
[3] Samantaray Arun K, Ould Bouamama Belkacem. Model-based process supervision: a bond graph approach. Springer; 2008.

[4] Won Chang-Hee. Comparative study of various control methods for attitude control of a LEO satellite. Aerospace Sci Technol 1999;3:323–33.
[5] Jan YW, Chiou JC. Attitude control system for ROCSAT-3 microsatellite: a conceptual design. Acta Astron 2005;56:439–52.
[6] Li J, Wang Z. Attitude dynamics of a liquid-filled spacecraft with a manipulator. Commun Nonlinear Sci Numer Simul 1997;2:26–30.
[7] Ozdemir U, Kavsaoglu MS. Linear and nonlinear simulations of aircraft dynamics using body axis systems. Aircraft Eng Aerospace Technol 2006;8:638–48.
[8] Wertz James R. Spacecraft attitude determination and control. Kluwer Academic Publishers; 1978.
[9] Kaplan Marshal H. Modern spacecraft dynamics and control. John Wiley and Sons; 1976.